Research Article/Civil and Sanitary Engineering https://doi.org/10.15446/ing.investig.101082

Study on Closely Spaced Asymmetric Footings Embedded in a Reinforced Soil Medium

Estudio de zapatas asimétricas poco espaciadas incrustadas en un medio de suelo reforzado

Anupkumar G. Ekbote[1] and Lohitkumar Nainegali[2]

ABSTRACT

In practice, footings are rarely laid on the surface or at ground level; usually, they are embedded in the soil medium. Most studies focus on surface footings. This research examines the behavior of two interfering asymmetric footings while considering their widths to be dissimilar and the effect of embedment depth to enhance the ultimate bearing capacity and limit the settlement within the working range. This was evaluated through the finite element method of the ABAQUS software. The soil was assumed to have a Mohr-Coulomb failure, and the asymmetry corresponded to the footing widths. The results are presented in terms of interference factors, *i.e.*, the ultimate bearing capacity (UBC) and the settlement, which are defined as the UBC/settlement ratio of the left/right footing in the presence of the other one placed on reinforced soil. This, in comparison with an identical isolated footing on unreinforced soil. Interference is more significant in small footings than in large ones. Due to behavioral variations, the bearing capacity and settlement are different. This effect increases with an increase in the width of large footings, and the interference factors decrease with an increase in the embedment depth of the footings. When the right footing width is twice that of the other and considering one layer of reinforcement and soil friction angles of 30° and 40°, the per-cent increments in the bearing capacity of interfering left footings, for a spacing of 0,5 times the left footing width, are 104 and 148%, respectively.

Keywords: interference, asymmetric footings, ultimate bearing capacity, settlement

RESUMEN

Las zapatas, en la práctica, rara vez se colocan en la superficie o al nivel del suelo; por lo general, están incrustadas en el medio del suelo. La mayoría de los estudios se centran en zapatas superficiales. Esta investigación examina el comportamiento de dos zapatas asimétricas que interfieren, considerando que sus anchos son diferentes y que el efecto de la profundidad de empotramiento mejora la capacidad portante última y limita el asentamiento dentro del rango de trabajo. Esto se evaluó a través del método de elementos finitos del *software* ABAQUS. Se asume la falla de Mohr-Coulomb en el suelo, y la asimetría corresponde al ancho de las zapatas. Los resultados se presentan en términos de factores de interferencia, *i.e.*, la capacidad portante última (UBC) y el asentamiento, que se definen como la relación de UBC/asentamiento de la zapata izquierda/derecha en presencia de la otra, colocada sobre suelo reforzado. Esto, en comparación con una zapata aislada idéntica sobre suelo no reforzado. La interferencia es más significativa en las zapatas pequeñas que en las grandes. Debido a las variaciones de comportamiento, la capacidad de carga y el asentamiento son distintos. Este efecto aumenta con el aumento del ancho las zapatas grandes, y los factores de interferencia disminuyen con el aumento de la profundidad de empotramiento de las zapatas. Cuando el ancho de la zapata derecha es el doble de la otra, y considerando una capa de refuerzo y ángulos de fricción del suelo de = 30° y 40°, el incremento porcentual en la capacidad portante de las zapatas izquierdas que interfieren, para un espaciamiento de 0,5 veces el ancho de la zapata izquierda, son 104 y 148 % respectivamente.

Palabras clave: interferencia, zapatas asimétricas, capacidad portante última, asentamiento

Received: February 16th, 2022
Accepted: May 8th, 2023

Introduction

Foundations, referred to as *sub-structures*, are an integral part of an engineered structural system. They safely transfer and distribute the load from the superstructure to the underlying soil/rock strata, so that neither the soil/rock fails in shear nor the foundation itself. The foundation/sub-structure constitutes an embedded part of the structure and acts as an intermediary between the superstructure and the ground on which the foundations are laid. The bearing capacity and the settlement characteristics of the underlying ground strata significantly govern the design of the foundation system and the structure's serviceability. The shear failure and or excessive settlement of the ground strata results in a distortion of the superstructure. Therefore, great attention must be paid to all the affecting factors.

[1] PhD, Indian Institute of Technology, Dhanbad. Affiliation: Assistant professor, Department of Civil Engineering, BMS Institute of Technology and Management, Yelahanka - 560064, Bengaluru, Karnataka, India. Email: anupge@gmail.com

[2] Corresponding Author, PhD, Indian Institute of Technology, Kanpur. Affiliation: Associate professor, Department of Civil Engineering, Indian Institute of Technology (ISM), Dhanbad, Dhanbad - 826004, Jharkhand, India. Email: lohitkumar@iitism.ac.in

Numerous studies have been conducted with the aim to predict the response of shallow foundations, and many pioneers (Prandtl, 1920; Terzaghi, 1943; Skempton, 1951; Meyerhof, 1963; Hansen, 1970; Vesic, 1773) have contributed to this theory. Thus, the expressions for estimating the bearing capacity and settlement aspects of shallow foundations resting on the soil and the rock strata have been derived. Notably, this theory and these equations are exceptionally valid for an isolated foundation system where no foundation exists in an isolated state. In several situations, individual or groups of foundations are persistently built in close proximity. Some of these situations include deficient construction space, restrictions in the property line, structural design requirements, and building architecture. Recently, with the increased expansion of infrastructures in conjunction with a rapid urbanization, and in order to tackle the problem of construction space, structures and sub-structures have been forced to come ever close to each other. In a way, foundations have been laid with closer spacing. Under such situations, the bearing capacity, settlement, failure mechanisms, and rotational characteristics are invariably different from those of isolated foundations. This may be due to the influence of one foundation on the other, as they are so closely laid. The stress isobars or the failure zones of neighboring foundations may combine or interfere with each other, leading to the phenomenon known as *foundation interference/interaction*. The overlapping of individual stress isobars or failure zones combines to form a single stress isobar or failure zone that extends both laterally and vertically, affecting large soil masses. This phenomenon alters the behavior of closely placed foundations when compared to the fundamental behavior of isolated ones, which also includes those that are placed far enough from each other so that may be considered to be isolated.

Many researchers have studied the problem by performing small-scale laboratory or field tests, as well as by conducting theoretical or numerical analyses on an unreinforced soil medium. These studies have implemented different theoretical or numerical techniques, such as a method of stress characteristics (Graham *et al*., 1984; Kumar and Ghosh, 2007a); upper bound limit analysis (Kumar and Kouzer, 2008; Kouzer and Kumar, 2008, 2010; Kumar and Ghosh, 2007b; Yang *et al*., 2017; Biswas and Ghosh, 2018; Keawsawasvong *et al*., 2021; Yodsomjai *et al*., 2021); lower bound limit analysis (Kumar and Bhattacharya, 2010, 2013; Shiau *et al*., 2021; Keawsawasvong and Boonchai Ukritchon, 2022); the finite difference method (Ghazavi and Lavasan, 2008; Ghosh and Sharma, 2010; Mabrouki *et al*., 2010; Lavasan and Ghazavi, 2012b; Javid *et al*., 2015; Lavasan *et al*., 2017); the finite element method (Lee *et al*., 2008; Lee and Eun, 2009; Kumar and Bhoi, 2010; Nainegali *et al*., 2013, 2018, 2019; Noorzad and Manavirad, 2014; Zidan and Mohamed, 2019; Sekhar *et al*., 2020; Shokoohi *et al*., 2019; Fuentes *et al*., 2019; Ekbote and Nainegali., 2019a, b; Sekhar *et al*., 2020; Alzabeebee, 2020, 2022; Ekbote *et al*., 2022); the analytical method (Kumar and Saran, 2003b, 2004; Ghosh *et al*., 2017); and the probabilistic approach (Griffiths *et al*., 2006).

In this vein, the ground improvement technique is a potentially cost-effective method, as it provides soil reinforcement for shallow foundations, constituting an alternative to conventional deep foundations wherever applicable. Soil reinforcement is carried out in several layers below the foundations, using geotextile, geogrid, geocell, or geocomposite materials. The use of reinforcement in the soil creates a composite material, increasing the bearing capacity and reducing the settlement of the foundations. Several numerical and experimental studies have been reported with regard to the effects of interference on reinforced soil beds. Moreover, several experimental studies on reinforced soil media have also been performed (Khing *et al*., 1992; Al-Ashou *et al*., 1994; Kumar and Saran, 2003a; Ghosh and Kumar, 2009; Lavasan and Ghazavi, 2012a; Naderi and Hataf, 2014; Gupta *et al*., 2018; Saha Roy and Deb 2018; Dehkordi *et al*., 2019; Paikaray *et al*., 2020; Swain and Ghosh, 2015). In this vein, an extensive state of the art review regarding the effect of interference on the behavior of shallow footings was carried out by Ghazavi and Dehkordi (2020).

Most of the studies reported in the literature deal with foundations identical in geometry and loading conditions (symmetrical planning). However, in many situations, structures located close to each other may have different configurations regarding their foundations; the shape of a foundation, as well as its size, may differ, and the super-structural load may be different. This gives rise to asymmetrical interference in the footings.

The subject of interference considering asymmetrical footings is rarely mentioned in the literature. Nainegali *et al*. (2013) highlighted the settlement of asymmetrical interfering strip footings laid on the surface of a linearly elastic non-homogeneous soil medium of finite and semi-infinite extent. Furthermore, they extended the study (Nainegali *et al*., 2018) to examine the interference effect on the bearing capacity and settlement of asymmetrical strip footings on the surface of a non-linearly elastic dense and loose sandy soil medium. In both studies, asymmetry affects the size of the footings, and the surcharge effect is not considered. Ghosh *et al*. (2017) examined the interference of two closely spaced asymmetric footings using the Pasternak model. They considered the hyperbolic stress-strain relation and performed linear and nonlinear elastic analyses. Ekbote and Nainegali (2021) studied two closely spaced asymmetric footings while considering different widths embedded in a homogenous, isotropic soil medium. The study focused on the effect of the width and embedment depth of the two footings, and its results align with earlier reports in conjunction with asymmetry. However, the embedment depth of the footings was also found to have a significant effect.

Most studies have been performed on surface footings, but, from a practical point of view, it is not viable to lay the foundation on the ground level (surface). Therefore, the reported literature does not give a clear picture of the interference effect on embedded footings.

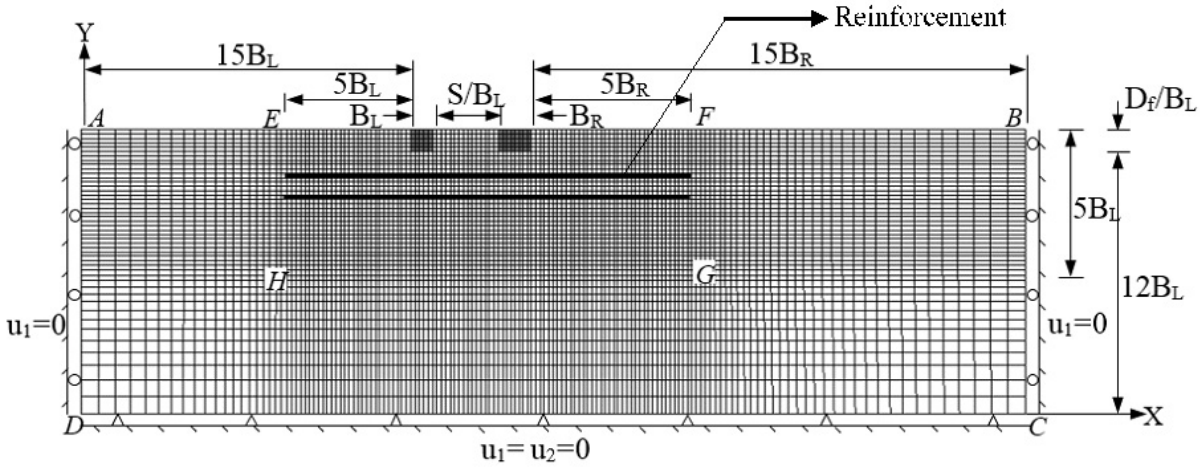

Figure 1. Problem domain along with associated boundary conditions
Source: Authors

For most structures, the foundations are laid below the ground surface (*i.e.*, embedded in nature). The overburden/surcharge from embedment amplifies the bearing capacity and reduces the settlement since there is an enhanced shearing zone. The literature on the effect of interference when footings are in a state of embedment in the reinforced soil medium is virtually null, and there is no study on the subject for embedded shallow footings. Therefore, this phenomenon must be analyzed. Moreover, bearing capacity and settlement are the primary criteria for shallow footing design, so, in order to overcome inadequacies and fill the research gap, this study focuses on these aspects of embedded shallow foundations resting on a reinforced soil medium while considering the embedment depth (same level).

Stating the problem

Figure 1 represents the problem domain, discretized using a structured finite element mesh and associated with appropriate boundary conditions. The problem considers two asymmetrical interfering strip footings with widths of B_L (left footing) and B_R (right footing), embedded at a depth D_f below the ground level, and laid with a clear spacing S. The footings are rigid, rough, and subjected to a load intensity q per-unit length of uniform load intensity. The foundation soil medium is assumed to be a homogeneous, isotropic, and semi-infinite cohesionless medium reinforced with a single and a double layer of geosynthetic material. The first layer (N = 1) of reinforcement is laid at a depth u below the base of the footings, and the consecutive layer (N = 2) at a depth h from the first reinforcement layer. The objective of this research is to perform a parametric study, varying contributing parameters such as the embedment depth of the footings (D_f), the width of the right footing (B_R), the soil friction angle (ϕ), the number of reinforcement layers, and the spacing between the footings (S). This works aims to explore the influence of the interference phenomenon on the behavior of asymmetrical footings (*i.e.*, ultimate bearing capacity, settlement, load-settlement response, and displacement pattern). Note that the right footing width is varied while the left footing width is kept constant. The range of varied parameters is shown in Table 1.

Table 1. Range of the parameters varied in the analyses

Parameters	Range considered for the analysis
B_R/B_L	1,5, and 2,0 (B_L = 1,0 m)
S/B_L	0,0; 0,25; 0,50; 0,75; 1,0; 1,5; 2,0; 3,0; 4,0; 5,0
D_f/B_L	0,25; 0,50; 0,75; 1,0
ϕ	25°; 30°; 35°; 40°
N	1; 2

Source: Authors

Methodology

The numerical analysis of the problem defined in the previous section employs the finite element method via the commercially available ABAQUS V6.13 software. The studied problem is regarded as a plane strain one since the footing length relative to the width is much higher. The interfering footings are considered asymmetrical with respect to the width of the footings, which are embedded at the same depth and loaded with the same magnitude. The width of the left footing is kept constant, and the width of the right interfering footing B_R is varied (Table 1). The Mohr-Coulomb failure criterion is used given its practical significance. It offers the best numerical approximation within the broad confining pressure range, as well as a trustworthy outcome for various nonlinear studies of the ground. Moreover, this criterion is used due to its mathematical simplicity and clear physical significance of the material parameters (Erickson and Drescher, 2002; Labuz and Zang, 2012). Accordingly, the soil medium is modeled as a linearly elastic, perfectly plastic material in compliance with the aforementioned

criterion (Ghazavi and Lavasan, 2008; Mabrouki *et al*., 2010; Shokoohi *et al*., 2018; Zidan and Mohamed, 2019; Sekhar *et al*., 2020). The footings embedded at the required depth are defined as a rigid and rough, linear elastic material (Vivek, 2011; Noorzad and Manavirad, 2014). The thickness of the footings equals their embedment depth. The reinforcement (geosynthetic) material behaves axially and as a linearly elastic material (Basudhar *et al*., 2007; Nazzal *et al*., 2010). The mechanical properties considered for the soil, the footings, and the reinforcement are specified in Table 2.

The foundation soil domain is discretized with structured meshing using two-dimensional plane strain linear continuum elements (CPE4R). A structured discretization meshing scheme is applied, which involves adopting fine mesh in the vicinity of high-stress concentration (around the interfering footings), as well as subsequent coarser meshing in the region of low-stress concentration, such as far-end boundaries. The dimensions are set after a sensitivity analysis regarding domain and mesh size and considering the accuracy of the results. The domain size considered in the analysis is presented in Figure 1. For the element size, elements with a uniform mesh of size 0,2 m are considered within a domain up to five times the width of the footing ($5B_L$) on either side (horizontal direction) and five times the width of the footing ($5B_L$) from the base (vertical direction). Thereupon, the elements vary from 0,2 to 0,8 m at the far-end boundaries using the single bias technique of the ABAQUS meshing module. A detailed mesh convergence study and a domain sensitivity analysis are presented in the recent article published by Ekbote and Nainegali (2021).

Table 2. Mechanical properties of the soil, footings, and reinforcement considered in the analysis

Parameters	Soil[$]	Footing*	Reinforcement (Geosynthetic)[#]
Young's Modulus (E), MPa	32	25x10^3	426
Poisson's ratio, υ	0,3	0,2	0,25
Cohesion (c), kPa	2	-	-
Soil friction angle (ϕ)	25° - 40°	-	-
Unit weight, kg/m^3	1 600	2 500	946

Source: $Mabrouki *et al*. (2010); *Vivek (2011); #Nazzal *et al*. (2010)

The geosynthetic reinforcement material is modeled as linearly elastic and discretized using two-dimensional quadratic truss elements (T2D3) that resist axial forces and do not resist any bending action. The reinforcement configuration is provided by optimizing the bearing capacity in order to obtain the maximum value. This is also done in Ekbote and Nainegali (2019a). Thus, the depth of the first layer of reinforcement u is 0,35 times B_L from the bottom of the footing, the distance between the first and the second layer h is 0,4 times B_L, and the length of reinforcement layer b is 5,0 times B_L. The interface between the soil and the footing, as well as between the soil and the reinforcement, is modeled using the interaction feature of ABAQUS (surface-to-surface, master-slave contact). Using this feature, there is a master and a slave surface. Defining such surfaces automatically generates a group of contact elements. The interaction simulation consists of normal-to-the-surface and tangential-to-the-surface components. The interface in the normal direction is assumed as hard contact with no separation allowed between the surfaces. The shear interactions are defined using Coulomb's friction law, by virtue of which a tangential behavior is defined between the contact surfaces a coefficient of friction μ, which is equal to the tangent of soil friction angle ϕ ($\mu = \tan \phi$). Appropriate boundary conditions essential for the solution approximation are established along the horizontal and vertical boundaries of the foundation soil domain. The suitable boundary conditions at the extreme boundaries are assigned in line with Potts and Zdravkovic (1999). Roller supports are considered along the far-end boundaries AD and BC in order to restrict the horizontal displacement ($u_1 = 0$) and allow any possible vertical displacement (u_2) at the far ends. Otherwise, the boundary DC is fixed to restrict horizontal and vertical displacements ($u_1 = u_2 = 0$).

Validation

This model was validated with the results of Nainegali *et al*. (2013, 2018). Nainegali *et al*. (2018) conducted a finite element analysis to study the settlement behavior of adjacent footings while considering the conditions of symmetry and asymmetry with respect to footing size and the applied loading with different combinations. Rough, rigid strip footings were placed on the surface of either a linearly elastic finite or an infinite non-homogeneous soil bed. Nainegali *et al*. (2013) presented their results in terms of the interference factor, which is the ratio of the average settlement of left/right footing in the presence of the right/left footing to that of the settlement of isolated footings. Nainegali *et al*. (2018) also performed a finite element analysis of two closely spaced strip footings on the surface of dense, loose, cohesionless soil beds. The footings were considered either symmetrical or asymmetrical based on their size. The soil was modeled following the non-linearly elastic soil, obeying the Duncan and Chang hyperbolic constitutive relationship. The results were presented in terms of interference factors such as the ratio of bearing pressure/settlement of interfering footings to that of isolated footings.

Table 3. Mechanical properties of soil considered for validation

Parameters	γ (kg/m^3)	E (kPa)	ν	c (kPa)	ϕ	ψ
Nainegali *et al*. (2013)	-	30x10^3	0,3	-	-	-
Nainegali *et al*. (2018)	1 700	30x10^3	0,3	0,1	36,5^0	0,1^0

Source: Nainegali *et al*. (2013, 2018)

The adopted model was validated by adopting the soil properties presented in Table 3 (Nainegali *et al*., 2013, 2018). The results of the comparison are presented in Figures 2a and 2b regarding Nainegali *et al*. (2013) and Nainegali *et al*. (2018), respectively. The variation was found to be similar and almost matching. However, a slight

difference was observed in our results, given the difference in the discretization scheme and the size of the elements considered. The differences in the computed interference factor at S/B_L = 0,50 for the left and right footings when compared to that of Nainegali *et al*. (2013) are 5 and 1%, respectively. Similarly, these differences, in comparison with Nainegali *et al*. (2018), are 1,5% and 1,9%, respectively. Overall, it can be seen that this finite element analysis model can be used reliably to address the aforementioned problem.

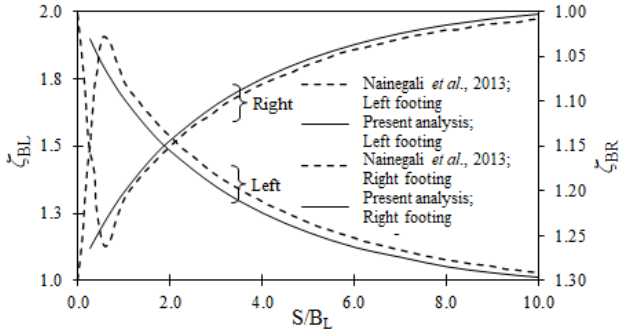

a) Comparison with Nainegali *et al*. (2013)

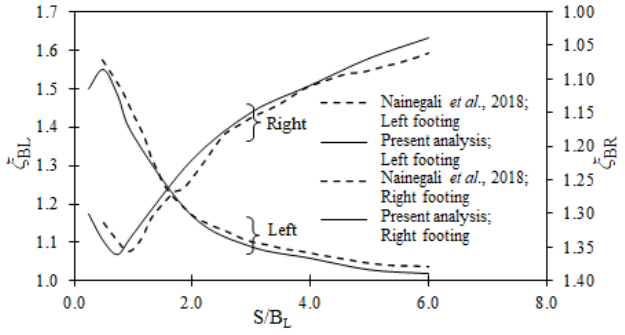

b) Comparison with Nainegali *et al*. (2018)
Figure 2. Results comparison with Nainegali *et al*. (2013, 2018)
Source: Authors

Results

A rigorous finite element analysis was performed to investigate the effect of interference on closely placed footings while considering asymmetry with respect to dimension (width), emphasizing the embedment of the footings in a geosynthetic reinforced soil medium. The analysis results regarding non-dimensional interference factors associated with the ultimate bearing capacity and the settlement were interpreted. The interference factor for the ultimate bearing capacity was estimated as defined in Equations (1a) and (1b) for the left and right footings, respectively. Similarly, the interference factor for the settlement was estimated according to the definitions given in Equations (2a) and (2b), for the left and right footings.

The permissible settlement (δ^p) is the maximum settlement allowed, irrespective of the footing type and size. As per the Indian Standard Code (IS 1904-1986), the maximum permissible settlement is 50 mm for isolated foundations in sand and hard clay for steel and reinforced concrete structures. The permissible bearing pressure (q^p) is the pressure corresponding to the δ^p assumed for an isolated footing. q^p (which corresponds to δ^p = 50mm) for different footing widths, depth of embedment, and soil friction angles was estimated, in the case of an unreinforced soil medium, by Ekbote and Nainegali (2021) (Table 4). These values are used to evaluate the interference factor for the settlement, as defined in Equations (2a) and (2b).

$$\xi_L^r = \frac{\text{Ultimate bearing capacity of the left footing in presence of the right footing embedded in reinforced soil medium}}{\text{Ultimate bearing capacity of an isolated footing identical to that of the left footing embedded in an unreinforced soil medium}} \quad (1a)$$

$$\xi_R^r = \frac{\text{Ultimate bearing capacity of the right footing in presence of the left footing embedded in reinforced soil medium}}{\text{Ultimate bearing capacity of an isolated footing identical to that of the right footing embedded in an unreinforced soil medium}} \quad (1b)$$

$$\zeta_L^r = \frac{\text{Settlement of the left footing embedded in reinforced soil medium (corresponding to permissible bearing pressure of an isolated footing same in size of the left footing, embedded in unreinforced soil medium)}}{\text{Permissible settlement}} \quad (2a)$$

$$\zeta_R^r = \frac{\text{Settlement of the right footing embedded in reinforced soil medium (corresponding to permissible bearing pressure of an isolated footing same in size of the right footing, embedded in unreinforced soil medium)}}{\text{Permissible settlement}} \quad (2b)$$

Table 4. Permissible bearing pressure q^p corresponding to the permissible settlement δ^p for an isolated footing

B	D_f/B_L	ϕ, (°)	q^p, kN/m	D_f/B_L	ϕ, (°)	q^p, kN/m
1,0	0,25	25	158,4	0,75	25	246,4
		30	279,3		30	362,6
		35	427,0		35	465,1
		40	528,3		40	521,4
	0,50	25	208,4	1,00	25	254,5
		30	337,1		30	369,6
		35	444,6		35	471,2
		40	533,4		40	492,9
1,5	0,25	25	185,1	0,75	25	229,7
		30	290,7		30	321,1
		35	373,8		35	396,0
		40	439,1		40	434,8
	0,50	25	210,9	1,00	25	233,5
		30	304,3		30	325,3
		35	380,7		35	399,9
		40	439,6		40	426,6
2,0	0,25	25	190,8	0,75	25	215,8
		30	272,8		30	294,3
		35	336,1		35	355,5
		40	386,8		40	386,1
	0,50	25	201,5	1,00	25	192,8
		30	279,5		30	298,4
		35	341,5		35	357,8
		40	388,3		40	375,6

Source: Ekbote and Nainegali (2021)

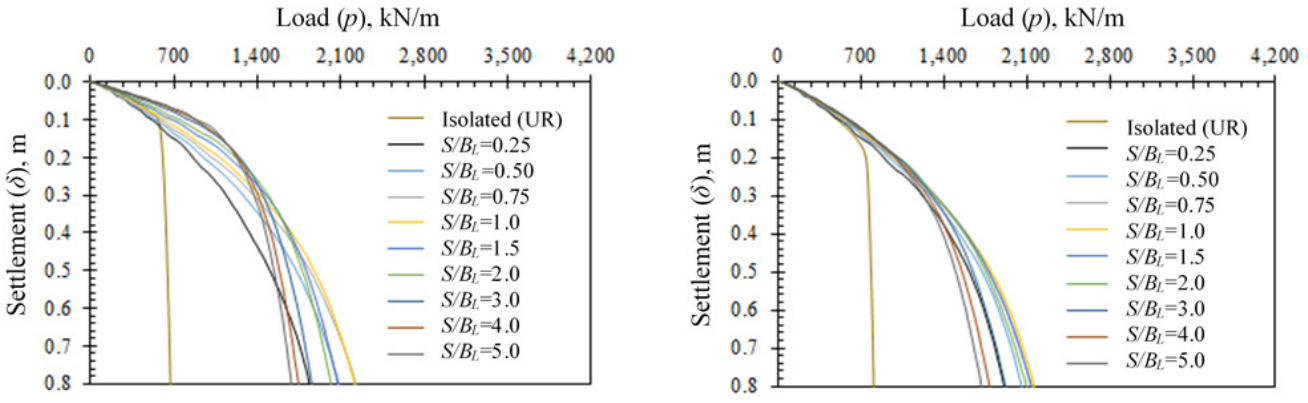

a) Left footing **b)** Right footing

Figure 3. p-δ plots for interfering asymmetric footings embedded in reinforced soil. D_f/B_L = 1,0, ϕ = 30°, B_R = 2,0B_L, N = 2.
Source: Authors

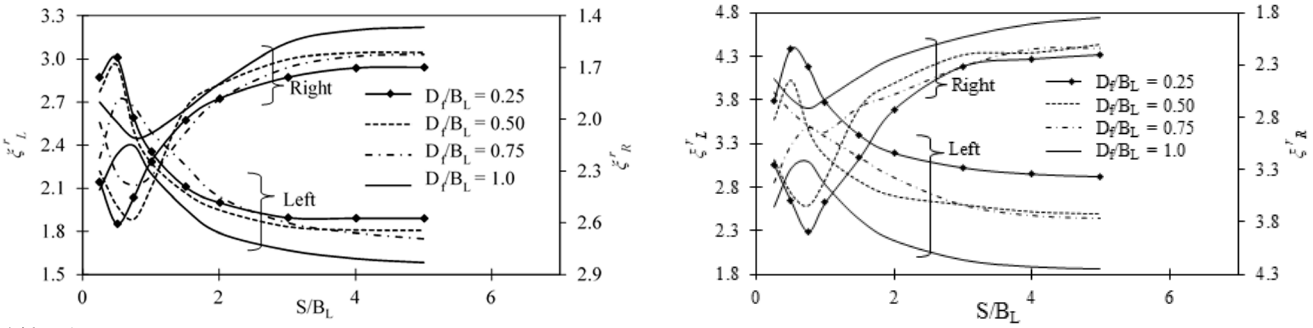

a) N = 1 **b)** N = 2

Figure 4. Variation of ξ_L^r and ξ_R^r with the S/B_L ratio for various D_f/B_L values in soil with ϕ = 30°: B_R = 1,5B_L
Source: Authors

The load-settlement (p-δ) response of the left and right asymmetrical interfering footings placed at different spacings (S/B_L ratio) for the case of B_R = 2,0B_L, embedded at depth, and D_f/B_L=1,0 in soil a having friction angle of ϕ=30° and reinforced with a single layer (N = 2) of reinforcement are illustrated in Figures 3a and 3b. The p-δ curve of the corresponding identical isolated footing embedded in an unreinforced soil bed (Isolated (UR)) is also shown in the figures for comparison. It can be noted that the response of asymmetrical interfering footings differs when compared to that of isolated ones. An explanation for the increased bearing capacity with a decreased footing spacing can be found in Stuart (1962). The load-carrying capacity increases with an increase in the number of reinforcement layers. The enhanced shear strength of the reinforced soil bed, which also increases with the number of reinforcing layers, is responsible for the higher load bearing capacity. According to Shukla (2021), the friction between the soil and the reinforcement layers primarily drives the reinforced soil's composite system. Additionally, the presence of or increase in reinforcement layers transforms the mechanism of soil shear failure into one of general shear failure (Guido *et al.*, 1985). From Figure 3, it can be stated that the p-δ curves of the interfering footings for spacings greater than 3,0 are more or less overlapping. This indicates that the interfering footings are starting to act as an isolated one. It cannot be ignored that there is a significant effect due to the asymmetry of the base (width of the adjacent base), *i.e.*, there is a behavioral difference in p-δ for both the left and the right footings. For the smaller left footing, the p-δ curves for different spacings are more distributed than those of the larger right footing.

By obtaining the bearing capacity from the load-settlement curves, the interference factors associated with the ultimate bearing capacity for the left footing (ξ_L^r) and the right footing (ξ_R^r) were evaluated for the range of parameters varied in the analysis, using Equations (1a) and (1b), respectively. The load-settlement curves obtained for the interfering footings do not show a definitive failure point. Therefore, in order to obtain the ultimate bearing capacity, a double-tangent method was used, referring to Naderi and Hataf (2014), Ghosh *et al.* (2015), and Saha Roy and Deb (2018). The variations in ξ_L^r and ξ_R^r with spacing (S/B_L ratio) for footing embedment at different depths (D_f/B_L ratio) in soil having a friction angle of ϕ = 30° for the case of B_R = 1,5B_L are presented in Figures 4a and 4b for single (N = 1) and double (N = 2) layers of reinforcement. The case of B_R = 2,0B_L is illustrated in Figures 5a and 5b. Similarly, Figures 6a and 6b, for N = 1 and 2, present these variations for the case of B_R

$= 1{,}5B_L$, footings embedded at $D_f/B_L = 1{,}0$, and different soil friction angles. The same is illustrated in Figures 7a and 7b for the case of $B_R = 2{,}0B_L$.

It can be observed, in Figures 4a, 4b, 5a, and 5b, that the footings embedded at smaller depths have higher interference factors. The interference factors of each footing are presented on either side of the figures. The peak interference factors ($\xi_L^{r,max}$ and $\xi_R^{r,max}$) decrease progressively with an increased embedment depth of the footings. Moreover, the peak interference factors increase with the soil friction angle. The spread of the plastic zone beneath the footing grows with an increase in soil friction angle, which is often related to an increasing shear strength. Additionally, when the soil friction angle increases, the failure pattern expands in the lateral and downward directions with increasing scope (Kouzer and Kumar, 2010; Yang *et al*., 2017). Furthermore, Figures 6a, 6b, 7a, and 7b show that the spacings at which the peak occurs increase for the right footing when compared to the left footing.

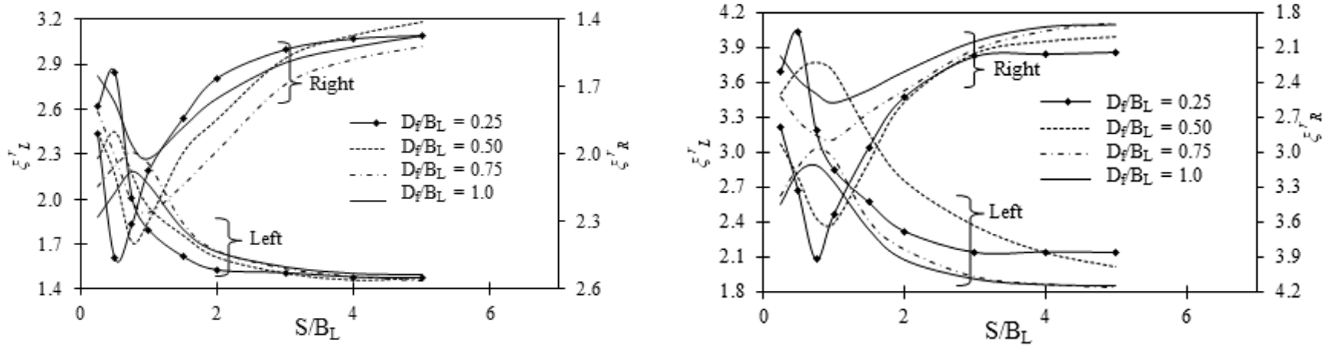

a) N = 1 **b)** N = 2

Figure 5. Variation of ξ_L^r and ξ_R^r with the S/B_L ratio for various D_f/B_L values in soil with $\phi = 30°$: $B_R = 2{,}0B_L$
Source: Authors

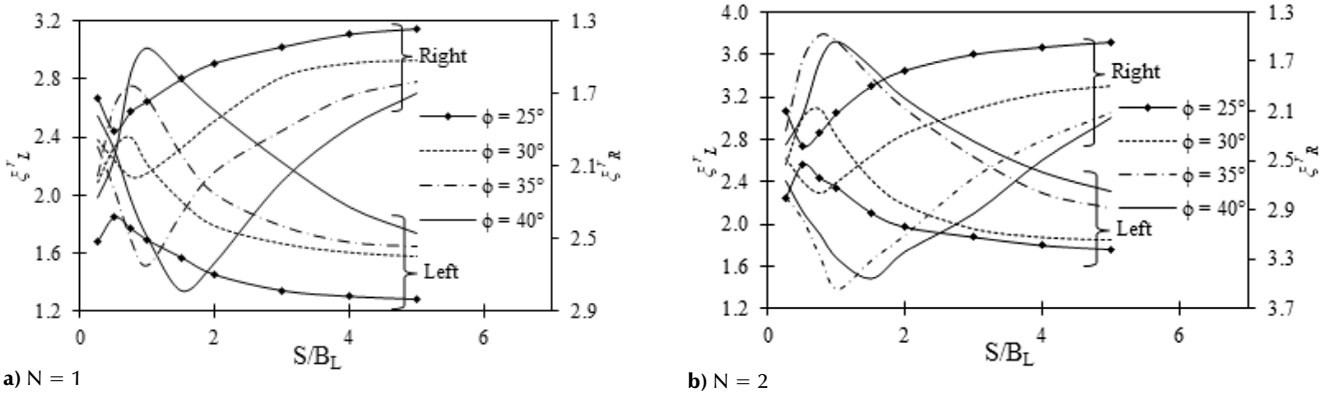

a) N = 1 **b)** N = 2

Figure 6. Variation of ξ_L^r and ξ_R^r with the S/B_L ratio for various soil friction angles at $D_f/B_L = 1{,}0$: $B_R = 1{,}5B_L$
Source: Authors

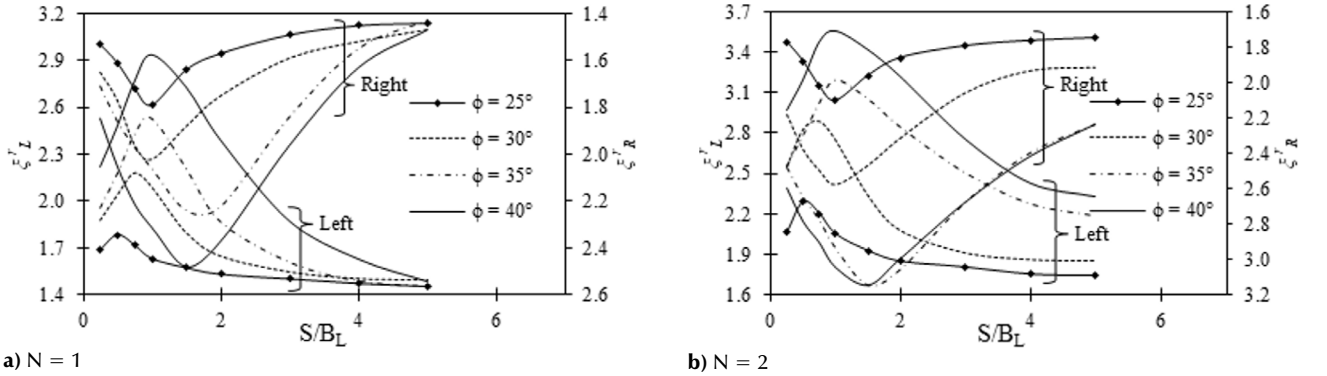

a) N = 1 **b)** N = 2

Figure 7. Variation of ξ_L^r and ξ_R^r with the S/B_L ratio for various soil friction angles at $D_f/B_L = 1{,}0$: $B_R = 2{,}0B_L$
Source: Authors

In Figures 4-7, knowing the interference factor, the percent increase in the bearing capacity of the interfering footings can be obtained in comparison with the corresponding isolated footing, *i.e.*, [(ξ_L^r or ξ_R^r – 1,0) x 100]. As an example, it can be noted that, for D_f/B_L = 1,0 for the left footing when B_R = 2,0B_L, placed with one layer of reinforcement (N = 1) and ϕ = 25°, 30°, 35°, and 40° the percent increase in the bearing capacity of the interfering footings at S/B_L = 0,50 is 78, 104, 118, and 148%, respectively, compared to their corresponding isolated footing. In the case of a specified angle of soil friction and spacing ratio, according to Equation (1), the interference factor increases with a decrease in the depth of the footing embedment. However, the load-carrying capacity of the soil increases with an increase in the embedment depth of the footing, due to an increased shearing zone and enhanced overburdening. The bearing capacity predominantly increases with an increase in the embedment depth for both isolated and interfering footings. As an example, consider a specified ϕ = 30° and S/B_L = 0,5 for the case B_R = 2,0B_L. The bearing capacity of the left footing when N = 1 increases from 104 to 185%, with a decrease in the depth of footing embedment from D_f/B_L = 1,0 to 0,25. The improvement in the ultimate bearing capacity for symmetrical interfering footings in a soil medium reinforced with N-layers of geosynthetic material is evident in earlier research on surface footings (Ghazavi and Lavasan, 2008; Lavasan *et al*., 2017; Biswas and Ghosh, 2018) and embedded footings (Ekbote and Nainegali, 2019a), which holds true in the case of asymmetric footings. However, $\xi_L^{r,max}$ is higher than $\xi_R^{r,max}$. The peak interference factors for N = 2 are shown in Table 5 for various embedment depths, soil friction angles, and footing widths. For the footings embedded at D_f/B_L = 1,0, the percentage difference in $\xi_L^{r,max}$ and $\xi_R^{r,max}$ for ϕ = 25°, 30°, 35° and 40° for B_R = 1,5B_L is 8,6, 12,3, 7,7, and 8,6%, respectively. Similarly, for B_R = 2,0B_L, these values are 8,3, 10,7, 1,6, and 11,5%, respectively. The percentage decrease in $\xi_L^{r,max}$ for N = 2, B_R = 2,0B_L when the embedment depth is increased from 0,25 to 1,0 for ϕ = 25°, 30°, 35° and 40° is 43,23, 39,44, 53,75, and 42,41%, respectively, and the percentage decrease in $\xi_R^{r,max}$ for ϕ = 25°, 30°, 35°, and 40° is 73, 52, 40, and 42%.

The settlement analysis of asymmetrical interfering footings embedded in a reinforced soil medium was carried out by evaluating the settlement at the bearing pressure corresponding to the permissible settlement of an isolated footing (50 mm) embedded in an unreinforced soil medium. The permissible bearing pressures corresponding to the permissible settlement for given values regarding the right footing width, embedment depth, and soil friction angle is shown in Table 4. Accordingly, the interference factors for the settlement of the left footing (ζ_L^r) are calculated using Equation (2a) and those for the right footing (ζ_R^r) using Equation (2b). The variations of ζ_L^r and ζ_R^r with spacings for N = 1 and 2 and the unreinforced case (N = 0) are presented in Figures 8a, 8b, 8c, and 8d for footings embedded at depths D_f/B_L = 0,25, 0,50, 0,75, and 1,0, respectively, with B_R = 1,5B_L and ϕ = 30°. The magnitude of the settlement interference factors of the left footings (ζ_L^r) are presented on the left-hand side of the figures, and those of the right footings (ζ_R^r) are presented on the right-hand side with values in reverse order. The width of the right footing (B_R = 2,0B_L) is shown in Figures 9a to d. Similarly, the variations of ζ_L^r and ζ_R^r with spacings for different soil friction angles (ϕ = 25°, 30°, 35°, and 40°) and D_f/B_L = 1,0 when B_R = 1,5B_L and B_R = 2,0B_L are presented in Figures 10a to d and 11a to d. The settlement interference factor continuously decreases with increased spacing between the footings for all the soil friction angles and embedding depths considered as the arching. The confinement effect of soil diminishes with the increasing proximity of the footings. The maximum settlement ($\zeta_L^{r,max}$ and $\zeta_R^{r,max}$) occurs at the minimum spacing considered (S/B_L = 0,25). However, the magnitude of the settlement decreases with an increase in both the embedment depth and the friction angle. The settlement was found to decrease further with the introduction of reinforcement layers, which is due to an increase in the shear strength of the soil.

The percentage decrease for the maximum settlement, given a footing width B_R = 1,5B_L, with N = 1 and ϕ = 30°, when the footing embedment depth is increased from D_f/B_L = 0,25 to 1,0, is 21% for the left footing and 20,7% for the right one. Similarly, the percentage decrease in the

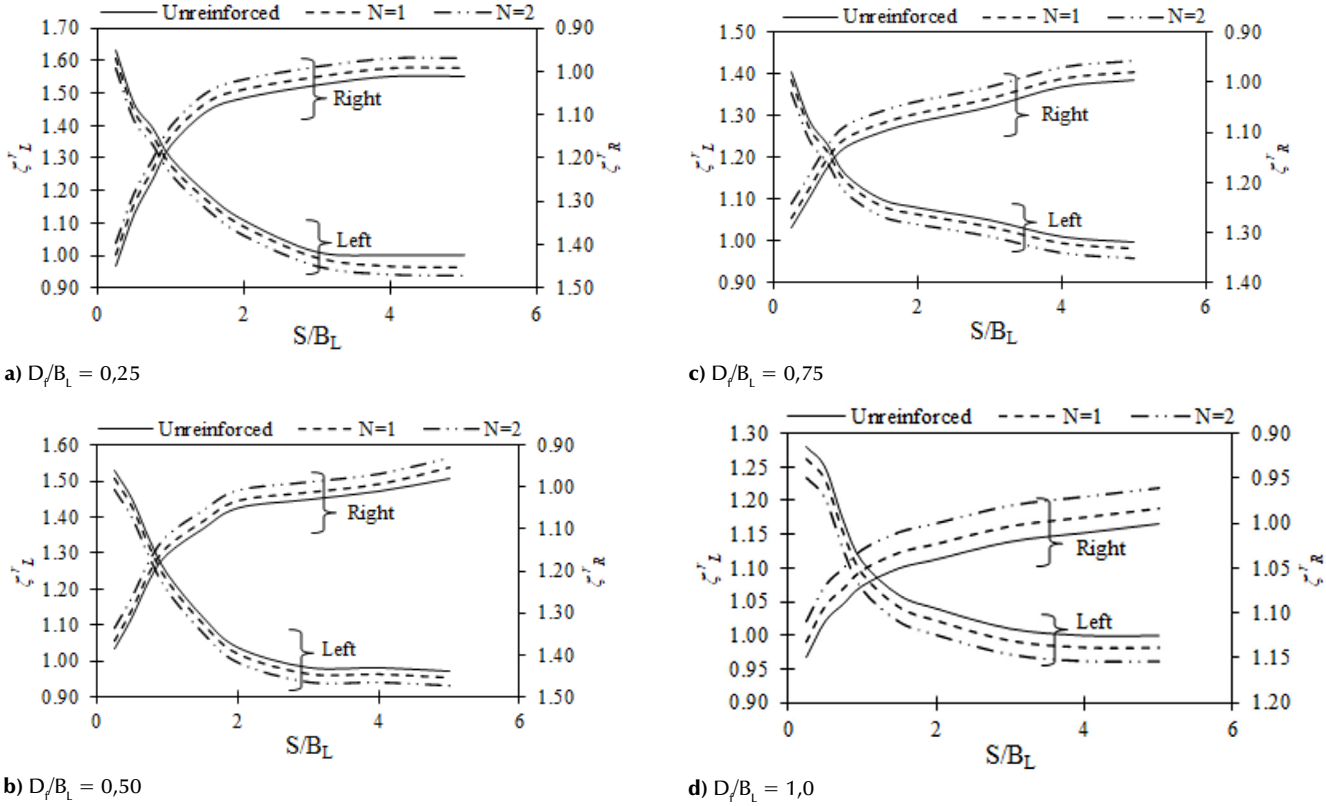

Figure 8. Variations in ζ_L^r and ζ_R^r with S/B_L ratio for N = 0 (unreinforced), 1, and 2 at different embedment depths in soil with ϕ = 30°: B_R = 1,5B_L
Source: Authors

maximum settlement when the embedment depth is increased from D_f/B_L = 0,25 to 1,0 for $B_R = 2{,}0B_L$, N = 1, and ϕ = 30° is 22,3% for the left footing and 20,9% for the right one. Furthermore, the decreases in the settlement when the soil friction angle is increased from ϕ = 25° to 40° for D_f/B_L = 1,0, $B_R = 1{,}5B_L$, and N = 1, for the left and right footings, respectively. These values (when $B_R = 2{,}0B_L$) are 14% for the left footing and 7,2% for the right one. Similarly, the decrease in the settlement when the soil friction angle is increased from ϕ = 25° to 40° for D_f/B_L = 1,0, $B_R = 1{,}5B_L$, and N = 2 is 11,1% (left footing) and 5,8% (right footing). For $B_R = 2{,}0B_L$, these values are 13,9 and 7,2%, respectively.

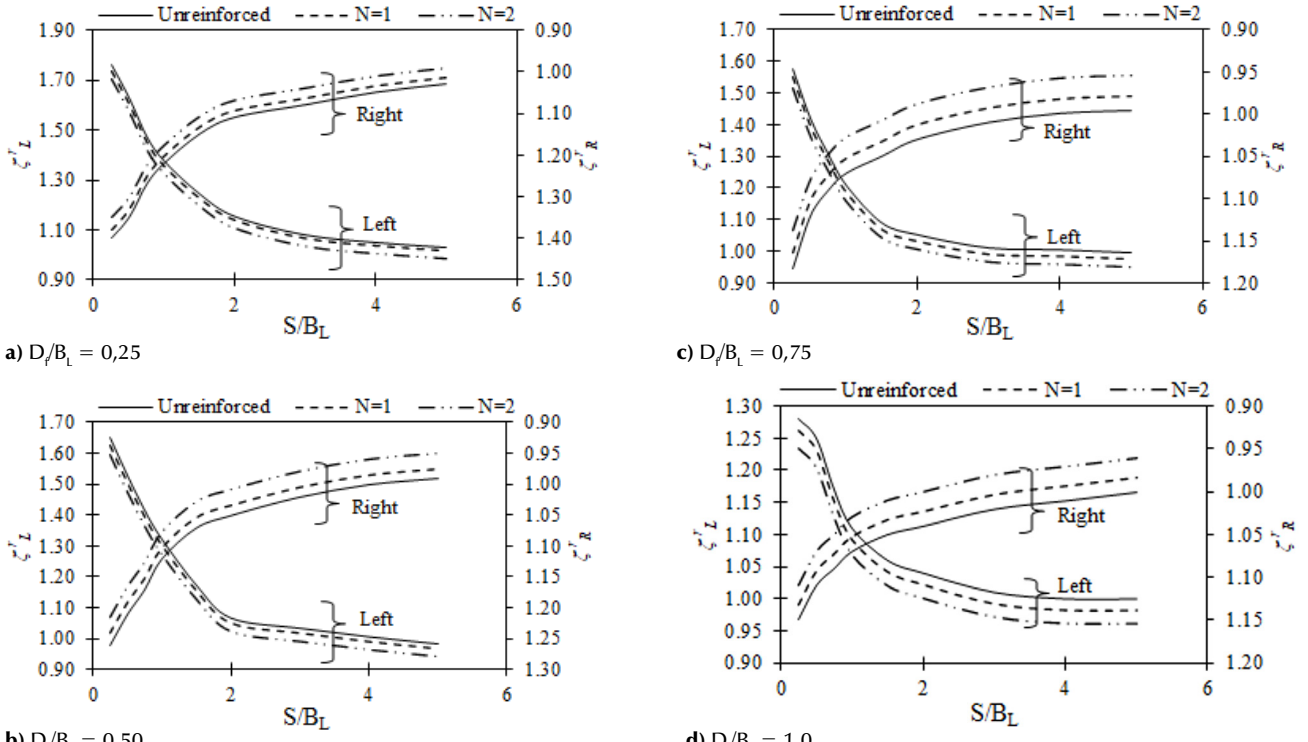

a) D_f/B_L = 0,25 **c)** D_f/B_L = 0,75

b) D_f/B_L = 0,50 **d)** D_f/B_L = 1,0

Figure 9. Variations in ζ_L^r and ζ_R^r with S/BL ratio for N = 0 (unreinforced), 1, and 2 at different embedment depths in soil with ϕ = 30°: BR = 2,0BL
Source: Authors

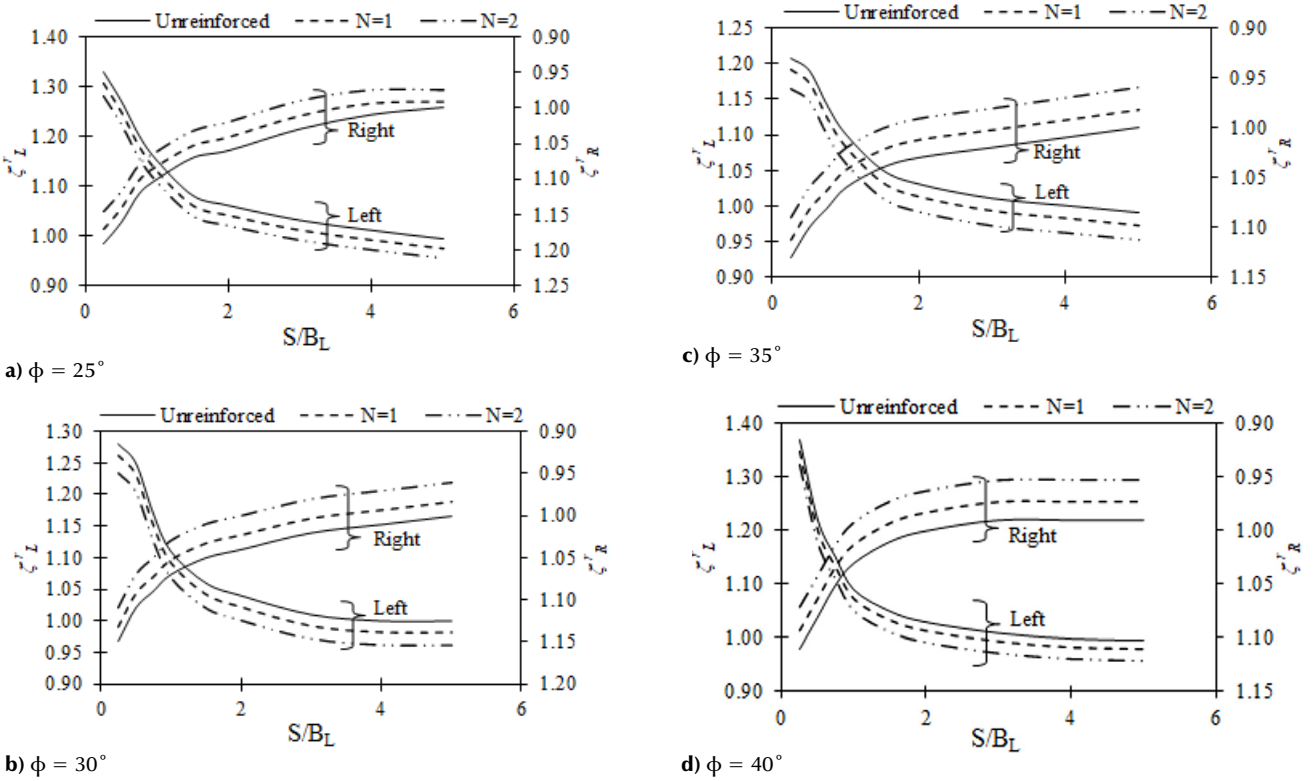

a) ϕ = 25° **c)** ϕ = 35°

b) ϕ = 30° **d)** ϕ = 40°

Figure 10. Variations in ζ_L^r and ζ_R^r with the S/B_L ratio for N = 0 (unreinforced), 1, and 2 in soil with different ϕ, with D_f/B_L = 1,0: $B_R = 1{,}5B_L$
Source: Authors

Table 5. Peak interference factors ($\xi_L^{r,max}$ and $\xi_R^{r,max}$) for different D_f/B_L, ϕ, and B_R/B_L values for two layers of reinforcement

D_f/B_L	ϕ	$B_R = 1,5B_L$		$B_R = 2,0B_L$		D_f/B_L	ϕ	$B_R = 1,5B_L$		$B_R = 2,0B_L$	
		$\xi_L^{r,max}$	$\xi_R^{r,max}$	$\xi_L^{r,max}$	$\xi_R^{r,max}$			$\xi_L^{r,max}$	$\xi_R^{r,max}$	$\xi_L^{r,max}$	$\xi_R^{r,max}$
0,25	25°	2,61	2,67	3,28	3,64	0,75	25°	2,69	2,65	2,62	2,21
	30°	4,39	3,89	4,03	3,92		30°	3,48	2,95	3,03	2,89
	35°	3,97	3,71	4,92	4,41		35°	3,89	3,59	3,78	3,36
	40°	5,14	4,97	5,07	4,42		40°	3,78	3,68	3,61	3,47
0,50	25°	2,92	2,70	2,67	2,44	1,0	25°	2,56	2,34	2,29	2,10
	30°	4,02	3,64	3,77	3,62		30°	3,09	2,71	2,89	2,58
	35°	4,00	3,68	3,89	3,73		35°	3,78	3,49	3,20	3,15
	40°	3,76	3,73	3,83	3,76		40°	3,72	3,40	3,56	3,15

Source: Authors

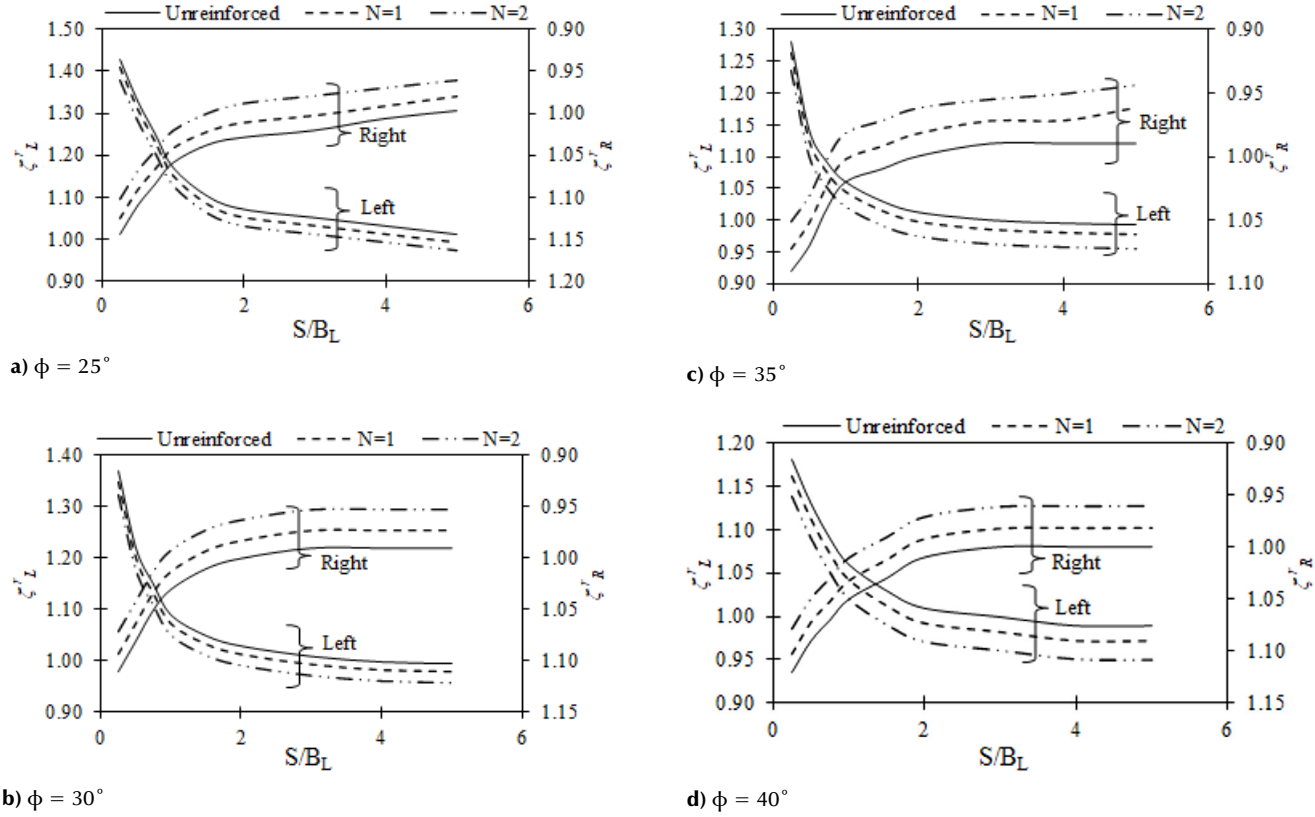

a) ϕ = 25°

c) ϕ = 35°

b) ϕ = 30°

d) ϕ = 40°

Figure 11. Variations in ζ_L^r and ζ_R^r with the S/B_L ratio for N = 0 (unreinforced), 1, and 2 in soil with different ϕ and D_f/B_L = 1,0: $B_R = 2,0B_L$
Source: Authors

The failure of the two closely placed asymmetrical footings can be visualized through the total displacement contour plots and is presented for $B_R = 2,0B_L$ and $D_f/B_L = 1,0$ in a soil medium (ϕ = 30°) with a double layer of geosynthetic reinforcement (Figures 12a, 12b, 12c, and 12d) for footings spaced at S/B_L = 0,25, 0,50, 1,0, and 5,0. The plots correspond to the ultimate bearing capacity. The displacement vectors are also shown over the plots to represent the direction and magnitude. Figures 12a to d show a general form of shear failure. It can be observed (Figures 12a and 2b) that the displacement vectors in between the two footings are absent, *i.e.*, the soil heave is not observed. This implies that adjacent footings with very close spacings (S/B_L = 0,25 and 0,50) act as one unit and relate to the single footing having a greater width (B_L+S/B_L+B_R). Furthermore, with an increase in spacing (Figure 12c), the heave between the footings is observed. However, this coincides with the passive zones of the close footings, and, at far away spacings (Figure 12d), the footings start behaving as independent ones. When the soil medium is reinforced, the zone between the two footings gets more confined than in unreinforced soil. Thus, the soil starts to densify until the shear failure occurs. The load carrying capacity was found to increase with a decrease in the settlement. The failure in the reinforced soil medium was assumed to be related to shear given a slip between the soil and the reinforcement (Basudhar *et al.*, 2008).

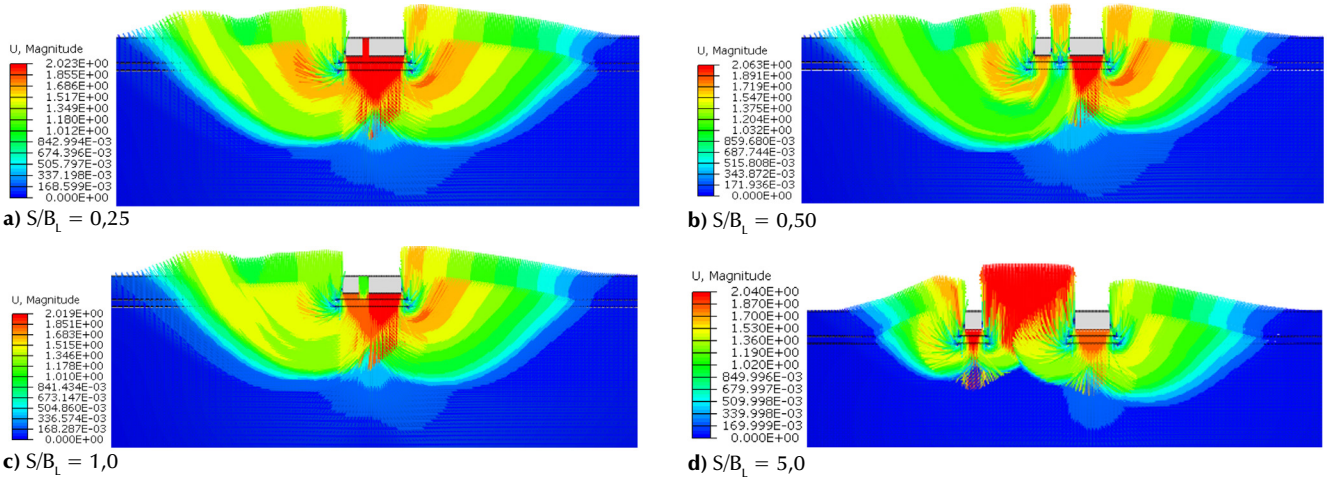

Figure 12. Total displacement contour plot for asymmetrical interfering footings on reinforced soil with $\phi = 30^{\circ}$ for $D_f/B_L = 1,0$, $B_R/B_L = 2,0$, and N = 2 at different S/B_L
Source: Authors

Conclusions

The performance of two closely spaced asymmetric footings embedded in a cohesionless reinforced foundation soil medium was studied using finite element analysis. Asymmetry was considered only with respect to the width of the footings, and thus the entire domain was used in the analysis while adopting appropriate boundary conditions. A sensitivity analysis for the domain and element size was performed, and the finite element model was validated with benchmark problems reported in the literature. The influence of the interference phenomenon on the load-settlement response, the ultimate bearing capacity, the settlement, and the displacement pattern was analyzed by varying several contributing parameters. Observations on the ultimate bearing capacity and the settlement were presented in terms of non-dimensional interference factors defined for this purpose. This study leads to the following conclusions:

- The effect of the interference phenomenon is significant, and its influence is asymmetry, that is, the influence of the large footing on the small adjacent one is predominant.
- The depth of footing embedment and the soil friction angle have a noteworthy influence on the interference effect.
- For a given depth of embedment, the peak interference factor associated with the ultimate bearing capacity increases with an increase in the soil friction angle. It also decreases with an increase in the embedment depth of the footing for a given value of soil friction angle.
- The interference factors associated with the ultimate bearing capacity for the reinforced soil medium (ξ_L^r and ξ_R^r) vary similarly to those of unreinforced soil with spacing between the footings.
- In comparison with the unreinforced soil medium, the settlement analysis for the reinforced soil medium (which considered the corresponding permissible limit) was found to follow a similar variation regarding the interference factors (ξ_L^r and ξ_R^r) and the spacing between the footings. However, the magnitudes were found to decrease, which accounts for the reduced settlement. Reductions in the settlement magnitude of 1,5 and 4,5% were noted for N = 1 and N = 2, respectively.

CRediT author statement

All authors: conceptualization, methodology, software, validation, formal analysis, investigation, writing (original draft, writing, review, and editing), data curation.

References

Al-Ashou, M. O., Sulaiman, R. M., and Mandal, J. N. (1994). Effect of number of reinforcing layers on the interference between footings on reinforced sand. *Indian Geotechnical Journal, 24*(3), 285-301.

Alzabeebee, S. (2020). Numerical analysis of the interference of two active machine foundations. *Geotechnical and Geological Engineering, 38*(5), 5043-5059. https://doi.org/10.1007/s10706-020-01347-w

Alzabeebee, S. (2022). Interference of surface and embedded three strip footings in undrained condition. *Transportation Infrastructure Geotechnology, 9*(2), 250-267. https://doi.org/10.1007/s40515-021-00172-9

Basudhar, P. K., Dixit, P. M., Gharpure, A., and Deb, K. (2008). Finite element analysis of geotextile-reinforced sand-bed subjected to strip loading. *Geotextiles and Geomembranes, 26*(1), 91-99. https://doi.org/10.1016/j.geotexmem.2007.04.002

Basudhar, P. K., Saha, S., and Deb, K. (2007). Circular footings resting on geotextile-reinforced sand bed. *Geotextiles and Geomembranes, 25*(6), 377-384. https://doi.org/10.1016/j.geotexmem.2006.09.003

Biswas, N., and Ghosh, P. (2018). Interaction of adjacent strip footings on reinforced soil using upper-bound limit analysis. *Geosynthetics International, 25*(6), 599-611. https://doi.org/10.1680/jgein.18.00020

Ekbote, A. G., and Nainegali, L. (2019a). Interference of two closely spaced footings embedded in unreinforced and reinforced soil medium: a finite element approach using ABAQUS. *Arabian Journal of Geosciences, 12*(22), 1-21. https://doi.org/10.1007/s12517-019-4868-0

Ekbote, A. G., and Nainegali, L. (2019b). Interference of two closely spaced strip footings embedded in cohesionless fibre-reinforced foundation soil bed. In American Society of Civil Engineers, *Geo-Congress 2019: Foundations* (pp. 454-464). American Society of Civil Engineers. https://doi.org/10.1061/9780784482094.041

Ekbote, A. G., and Nainegali, L. (2021). Finite element analysis of two nearby interfering asymmetric footings embedded in cohesionless foundation medium. *Geomechanics and Geoengineering, 16*(4), 263-276. https://doi.org/10.1080/17486025.2019.1664776

Ekbote, A. G., Nainegali, L., Rajhans, P., and Deepak, M. S. (2022). Behavioural assessment on influence of adjacently placed strip footings at different embedment level. *Architecture, Civil Engineering, Environment, 15*(4), 93-103. https://doi.org/10.2478/ACEE-2022-0041

Erickson, H. L., and Drescher, A. (2002). Bearing capacity of circular footings. *Journal of Geotechnical and Geoenvironmental Engineering, 128*(1), 38-43. http://ojps.aip.org/gto

Fazeli Dehkordi, P., Ghazavi, M., Ganjian, N., and Karim, U. F. A. (2021). Parametric study from laboratory tests on twin circular footings on geocell-reinforced sand. *Scientia Iranica, 28*(1), 96-108. https://doi.org/10.24200/SCI.2019.51471.2208

Fuentes, W., Duque, J., Lascarro, C., and Gil, M. (2019). Study of the bearing capacity of closely spaced square foundations on granular soils. *Geotechnical and Geological Engineering, 37*(3), 1401-1410. https://doi.org/10.1007/s10706-018-0694-5

Ghazavi, M., and Lavasan, A. A. (2008). Interference effect of shallow foundations constructed on sand reinforced with geosynthetics. *Geotextiles and Geomembranes, 26*(5), 404-415. https://doi.org/10.1016/j.geotexmem.2008.02.003

Ghosh, P., and Kumar, P. (2009). Interference effect of two nearby strip footings on reinforced sand. *Contemporary Engineering Sciences, 2*(12), 577-592. http://m-hikari.com/ces/ces2009/ces9-12-2009/ghoshCES9-12-2009.pdf

Ghosh, P., and Sharma, A. (2010). Interference effect of two nearby strip footings on layered soil: theory of elasticity approach. *Acta Geotechnica, 5*(3), 189-198. https://doi.org/10.1007/s11440-010-0123-2

Ghosh, P., Basudhar, P. K., Srinivasan, V., and Kunal, K. (2015). Experimental studies on interference of two angular footings resting on surface of two-layer cohesionless soil deposit. *International Journal of Geotechnical Engineering, 9*(4), 422-433. https://doi.org/10.1179/1939787914Y.0000000080

Ghosh, P., Rajesh, S., and Sai Chand, J. (2017). Linear and nonlinear elastic analysis of closely spaced strip foundations using Pasternak model. *Frontiers of Structural and Civil Engineering, 11*(2), 228-243. https://doi.org/10.1007/s11440-010-0123-2

Graham, J., Raymond, G. P., and Suppiah, A. (1984). Bearing capacity of three closely-spaced footings on sand. *Geotechnique, 34*(2), 173-181. https://doi.org/10.1680/geot.1984.34.2.173

Griffiths, D. V., Fenton, G. A., and Manoharan, N. (2006). Undrained bearing capacity of two-strip footings on spatially random soil. *International Journal of Geomechanics, 6*(6), 421-427. https://doi.org/10.1061/(ASCE)1532-3641(2006)6:6(42

Guido, V. A., Biesiadecki, G. L., and Sullivan, M. J. (1985). *Bearing capacity of a geotextile-reinforced foundation* [Conference presentation]. Proceedings of the Eleventh International Conference on Soil Mechanics and Foundation Engineering, San Francisco, CA, USA. https://www.issmge.org/uploads/publications/1/34/1985_03_0134.pdf

Gupta, A., Lakshman, G. K., and Sitharam, T. (2018). *Interference of square footings on geocell reinforced clay bed: Experimental and numerical studies* [Conference presentation]. 3rd World Congress on Civil, Structural, and Environmental Engineering (CSEE'18), Budapest, Hungary. https://doi.org/10.11159/icgre18.142

Hansen, B. J. (1970). *A revised and extended formula for bearing capacity. No. 28*. Danish Geotechnical Institute. https://trid.trb.org/view/125129

Hill, R. (1950). *The mathematical theory of plasticity*. Oxford University Press. https://global.oup.com/academic/product/the-mathematical-theory-of-plasticity-9780198503675?cc=in&lang=en&

IS 1904-1986 (Reaffirmed 2006). *Indian standard code of practice for design and construction of foundations in soils: General requirements*. Bureau of Indian Standards. https://law.resource.org/pub/in/bis/S03/is.1904.1986.pdf

Javid, A. H., Fahimifar, A., and Imani, M. (2015). Numerical investigation on the bearing capacity of two interfering strip footings resting on a rock mass. *Computers and Geotechnics, 69*, 514-528. https://doi.org/10.1016/j.compgeo.2015.06.005

Keawsawasvong, S., and Ukritchon, B. (2022). Design equation for stability of a circular tunnel in anisotropic and heterogeneous clay. *Underground Space, 7*(1), 76-93. https://doi.org/10.1016/j.undsp.2021.05.003

Keawsawasvong, S., Thongchom, C., and Likitlersuang, S. (2021). Bearing capacity of strip footing on Hoek-Brown rock mass subjected to eccentric and inclined loading. *Transportation Infrastructure Geotechnology, 8*, 189-202. https://doi.org/10.1007/s40515-020-00133-8

Khing, K. H., Das, B. M., Yen, S. C., Puri, V. K., and Cook, E. E. (1992). Interference effect of two closely-spaced shallow strip foundations on geogrid-reinforced sand. *Geotechnical and Geological Engineering, 10*(4), 257-271. https://doi.org/10.1007/BF00880704

Kouzer, K. M., and Kumar, J. (2008). Ultimate bearing capacity of equally spaced multiple strip footings on cohesionless soils without surcharge. *International Journal for Numerical and Analytical Methods in Geomechanics, 32*(11), 1417-1426. https://doi.org/10.1002/nag.677

Kouzer, K. M., and Kumar, J. (2010). Ultimate bearing capacity of a footing considering the interference of an existing footing on sand. *Geotechnical and Geological Engineering, 28*(4), 457-470. https://doi.org/10.1007/s10706-010-9305-9

Kumar, A., and Saran, S. (2003a). Closely spaced footings on geogrid-reinforced sand. *Journal of Geotechnical and Geoenvironmental Engineering, 129*(7), 660-664. https://doi.org/10.1061/(ASCE)1090-0241(2003)129:7(660)

Kumar, A., and Saran, S. (2003b). Closely spaced strip footings on reinforced sand. *Geotechnical Engineering, 34*(3), 177-186.

Kumar, A., and Saran, S. (2004). Closely spaced rectangular footings on reinforced sand. *Geotechnical and Geological Engineering, 22*(4), 497-524. https://doi.org/10.1023/B:GEGE.0000047041.52563.49

Kumar, J., and Bhattacharya, P. (2010). Bearing capacity of interfering multiple strip footings by using lower bound finite elements limit analysis. *Computers and Geotechnics, 37*(5), 731-736. https://doi.org/10.1016/j.compgeo.2010.05.002

Kumar, J., and Bhattacharya, P. (2013). Bearing capacity of two interfering strip footings from lower bound finite elements limit analysis. *International Journal for Numerical and Analytical Methods in Geomechanics, 37*(5), 441-452. https://doi.org/10.1002/nag.1104

Kumar, J., and Bhoi, M. (2010). Effect of interference of strip footings and strip anchors on their elastic settlements. *International Journal of Geotechnical Engineering, 4*(2), 289-297. https://doi.org/10.3328/IJGE.2010.04.02.289-297

Kumar, J., and Ghosh, P. (2007). Ultimate bearing capacity of two interfering rough strip footings. *International Journal of Geomechanics, 7*(1), 53-62. https://doi.org/10.1061/(ASCE)1532-3641(2007)7:1(5

Kumar, J., and Ghosh, P. (2007a). Upper bound limit analysis for finding interference effect of two nearby strip footings on sand. *Geotechnical and Geological Engineering, 25*(5), 499-507. https://doi.org/10.1007/s10706-007-9124-9

Kumar, J., and Kouzer, K. M. (2008). Bearing capacity of two interfering footings. *International Journal for Numerical and Analytical Methods in Geomechanics, 32*(3), 251-264. https://doi.org/10.1002/nag.625

Lavasan, A. A., and Ghazavi, M. (2012). Behavior of closely spaced square and circular footings on reinforced sand. *Soils and Foundations, 52*(1), 160-167. https://doi.org/10.1016/j.sandf.2012.01.006

Lavasan, A. A., and Ghazavi, M. (2016). Failure mechanism and soil deformation pattern of soil beneath interfering square footings. *Journal of Numerical Methods in Civil Engineering, 1*(2), 48-56. https://doi.org/10.29252/NMCE.1.2.48

Lavasan, A. A., Ghazavi, M., and Schanz, T. (2017). Analysis of interfering circular footings on reinforced soil by physical and numerical approaches considering strain-dependent stiffness. *International Journal of Geomechanics, 17*(11), 04017096. https://doi.org/10.1061/(ASCE)GM.1943-5622.000099

Lavasan, A. A., Ghazavi, M., von Blumenthal, A., and Schanz, T. (2018). Bearing capacity of interfering strip footings. *Journal of Geotechnical and Geoenvironmental Engineering, 144*(3), 04018003. https://doi.org/10.1061/(ASCE)GT.1943-5606.0001824

Lee, J., and Eun, J. (2009). Estimation of bearing capacity for multiple footings in sand. *Computers and Geotechnics, 36*(6), 1000-1008. https://doi.org/10.1016/j.compgeo.2009.03.009

Lee, J., Eun, J., Prezzi, M., and Salgado, R. (2008). Strain influence diagrams for settlement estimation of both isolated and multiple footings in sand. *Journal of Geotechnical and Geoenvironmental Engineering, 134*(4), 417-427. https://doi.org/10.1061/(ASCE)1090-0241(2008)134:4(417)

Mabrouki, A., Benmeddour, D., Frank, R., and Mellas, M. (2010). Numerical study of the bearing capacity for two interfering strip footings on sands. *Computers and Geotechnics, 37*(4), 431-439. https://doi.org/10.1016/j.compgeo.2009.12.007

Meyerhof, G. G. (1963). Some recent research on the bearing capacity of foundations. *Canadian Geotechnical Journal, 1*(1), 16-26. https://doi.org/10.1139/t63-003

Naderi, E., and Hataf, N. (2014). Model testing and numerical investigation of interference effect of closely spaced ring and circular footings on reinforced sand. *Geotextiles and Geomembranes, 42*(3), 191-200. https://doi.org/10.1016/j.geotexmem.2013.12.010

Nainegali, L. S., Basudhar, P. K., and Ghosh, P. (2013). Interference of two asymmetric closely spaced strip footings resting on non-homogeneous and linearly elastic soil bed. *International Journal of Geomechanics, 13*(6), 840-851. https://doi.org/10.1061/(ASCE)GM.1943-5622.0000290

Nainegali, L., Basudhar, P. K., and Ghosh, P. (2018). Interference of strip footings resting on non-linearly elastic foundation bed: a finite element analysis. Iranian *Journal of Science and Technology, Transactions of Civil Engineering, 42*(2), 199-206. https://doi.org/10.1007/s40996-018-0094-3

Nainegali, L., Basudhar, P. K., and Ghosh, P. (2021). Interference of proposed footing with an existing footing resting on non-linearly elastic dense and loose cohesionless soil bed. *European Journal of Environmental and Civil Engineering, 25*(14), 2574-2591. https://doi.org/10.1080/19648189.2019.1638311

Nazzal, M. D., Abu-Farsakh, M. Y., and Mohammad, L. N. (2010). Implementation of a critical state two-surface model to evaluate the response of geosynthetic reinforced pavements. *International Journal of Geomechanics, 10*(5), 202-212. https://doi.org/10.1061/(ASCE)GM.1943-5622.0000058

Noorzad, R., and Manavirad, E. (2014). Bearing capacity of two close strip footings on soft clay reinforced with geotextile. *Arabian Journal of Geosciences, 7*(2), 623-639. https://doi.org/10.1007/s12517-012-0771-7

Paikaray, B., Das, S. K., and Mohapatra, B. G. (2021). Effect of reinforcement layout on interference effect of square footings on reinforced crusher dust. *International Journal of Geotechnical Engineering, 15*(10), 1268-1277. https://doi.org/10.1080/19386362.2020.1712531

Potts, D.M. and Zdravkovic, L. (1999). *Finite element analysis in geotechnical engineering: Theory/application*. Thomas Telford. https://www.icevirtuallibrary.com/doi/book/10.1680/feaiget.27534

Prandtl, L. (1920). Ü̈ber die Härte plastischer Körper. *Nachrichten von der Gesellschaft der Wissenschaften zu Göttingen, Mathematisch-Physikalische Klasse, 1920*(1920), 74-85. https://eudml.org/doc/59075

Saha Roy, S., and Deb, K. (2018). Closely spaced rectangular footings on sand over soft clay with geogrid at the interface. *Geosynthetics International, 25*(4), 412-426. https://doi.org/10.1680/jgein.18.00025

Sekhar, J. C., Sasmal, S. K., and Behera, R. N. (2020). Effect of interference on ultimate bearing capacity of strip footings resting over multi-layered-reinforced soil. *Australian Journal of Multi-Disciplinary Engineering, 16*(1), 31-42. https://doi.org/10.1080/14488388.2020.1733739

Shiau, J., Chudal, B., Mahalingasivam, K., and Keawsawasvong, S. (2021). Pipeline burst-related ground stability in blowout condition. *Transportation Geotechnics, 29*, 100587. https://doi.org/10.1016/j.trgeo.2021.100587

Shokoohi, M., Veiskarami, M., and Hataf, N. (2019). A numerical and analytical study on the bearing capacity of two neighboring shallow strip foundations on sand. Iranian *Journal of Science and Technology, Transactions of Civil Engineering, 43*(1), 591-602. https://doi.org/10.1007/s40996-018-0189-x

Shukla, S. K. (Ed.). (2021). *ICE handbook of geosynthetic engineering: Geosynthetics and their applications*. ICE Publishing. https://www.icevirtuallibrary.com/doi/abs/10.1680/hge.41752

Skempton, A.W. (1951). *The bearing capacity of clay*. Building Research Congress. https://www.u-cursos.cl/ingenieria/2009/2/CI52Q/1/material_docente/bajar?id_material=244428

Stuart, J. G. (1962). Interference between foundations, with special reference to surface footings in sand. *Geotechnique, 12*(1), 15-22. https://doi.org/10.1680/geot.1962.12.1.15

Swain, A., and Ghosh, P. (2015). Experimental study on dynamic interference effect of two closely spaced machine foundations. *Canadian Geotechnical Journal, 53*(2), 196-209. https://doi.org/10.1139/cgj-2014-0462

Terzaghi, K. (1943). *Theoretical Soil Mechanics*. John Wiley and Sons. https://doi.org/10.1002/9780470172766

Vesić, A. S. (1973). Analysis of ultimate loads of shallow foundations. *Journal of the Soil Mechanics and Foundations Division, 99*(1), 45-73. https://doi.org/10.1061/JSFEAQ.0001846

Vivek, P. (2011). Static and dynamic interference of strip footings in layered soil [Master's dissertation, Indian Institute of Technology]. https://www.iitk.ac.in/ce/geotech/geotech_lab_iitkanpur_017.htm

Yang, F., Zheng, X. C., Sun, X. L., and Zhao, L. H. (2017). Upper-bound analysis of Nγ and failure mechanisms of multiple equally spaced strip footings. *International Journal of Geomechanics, 17*(9), 06017016. https://doi.org/10.1061/(ASCE)GM.1943-5622.0000984

Yodsomjai, W., Keawsawasvong, S., and Likitlersuang, S. (2021). Stability of unsupported conical slopes in Hoek-Brown rock masses. *Transportation Infrastructure Geotechnology, 8*, 279-295. https://doi.org/10.1007/s40515-020-00137-4

Zidan, A. F., and Mohamed, M. (2019). Numerical analysis of bearing capacity of multiple strip footing on unreinforced and reinforced sand beds. *SN Applied Sciences, 1*(11), 1-13. https://doi.org/10.1007/s42452-019-1520-2